Ionization Mechanism of Rydberg Atoms in a Circularly Polarized Microwave Field

David Farrelly

Department of Chemistry and Biochemistry, Utah State University, Logan, Utah 84322-0300

T. Uzer

School of Physics, Georgia Institute of Technology, Atlanta, Georgia 30332-0430

Placing a hydrogen atom in a circularly polarized microwave field exposes it to velocity-dependent forces that open new routes to chaotic ionization, access to which is controlled by the details of state preparation.

The recognition that relatively simple classical systems can display extraordinarily complicated motions has altered the direction of many areas of physics, ranging from celestial mechanics to atomic, molecular, and nuclear physics [1]. Rydberg atoms hold especial promise for unraveling the relationship between classically chaotic motion and quantum mechanics, and, to this end, powerful experimental and theoretical methods are being developed and applied to this problem. While most of the systems [2,3] studied so far represent problems in which a clear separation of the Hamiltonian into kinetic and potential parts is possible, recent ground-breaking experiments have started to focus on a broader class of problem in which the equations of motion contain velocity-dependent Coriolis-like terms, for instance, Rydberg atoms in crossed electric and magnetic fields [4], and, the subject of this Letter, the ionization of Rydberg states by circularly polarized (CP) microwave fields [5–7].

This Letter develops a mechanism that explains how the mixing of coordinates and momenta in the Coriolis term modifies considerably the ionization mechanism of Rydberg atoms in CP fields as compared to the well understood cases of static field and linearly polarized (LP) microwave field ionization [2]. In particular, we show that the dynamics is controlled by two critical points; associated with one is a bifurcation in the Hamiltonian flow that has a celestial counterpart in a similar bifurcation associated with Jupiter's Trojan asteroids [8,9]. Our analysis leads to an unambiguous definition of the ionization threshold and has the further merit of accounting for difficulties that have previously been reported in predicting this threshold [5,6]. Moreover, given the importance of Coriolis effects in many other fields, e.g., nuclear physics, molecular physics, and asteroid and satellite dynamics, the CP problem emerges as an important experimental and theoretical test bed with potentially far reaching applications [10,11].

We specialize in the planar CP problem which captures the essence of the three-dimensional ionization dynamics [6]. In Cartesian coordinates and atomic units the planar $(z = P_z = 0)$ CP Hamiltonian is [5–7]

$$H = E = \tfrac{1}{2}(p_x^2 + p_y^2) - \tfrac{1}{r} + F[x\cos\omega t + y\sin\omega t]. \quad (1)$$

The explicit time dependence may be removed by transforming to a synodic frame (x', y') rotating with frequency ω yielding the Hamiltonian

$$K = \tfrac{1}{2}(p_x^2 + p_y^2) - \tfrac{1}{r} - \omega\ell_z + Fx, \quad (2)$$

where $\ell_z = xp_y - yp_x$ and the primes have been dropped. The only exact invariant for the system, the quantity K, resembles the Jacobi constant of celestial mechanics [12], and will be referred to as such. While the dynamics is best studied by integrating Hamilton's equations of motion for K, ideally, one would prefer to integrate an ensemble of initial conditions having the same Keplerian energy E and a variety of ℓ_z values. This must be kept in mind when examining surfaces of section, which by necessity are computed at fixed K and thus contain trajectories having different initial values of E and ℓ_z but which do not reflect an experimentally prepared ensemble. Naturally, this complicates the connection between theoretical results in the rotating frame and actual experiments: Consider an ensemble of predominantly low ℓ_z states spanning a narrow range of E as is typically prepared in an experiment. Associated with each ℓ_z (and hence K) value in the selected n-manifold is a Kepler ellipse. As the CP field is turned on, each point on the Kepler ellipse will, in general, evolve into a different orbit in the rotating frame since neither $E = -1/2n^2$ nor ℓ_z are conserved. In the rotating frame, therefore, each trajectory in the resulting ensemble will have a different value of K. This argument, which is supported by extensive numerical simulations, suggests that the experimental distribution of states and, consequently, the ionization mechanism, will depend strongly on the manner in which the CP field is turned on.

Although the mixing of coordinates with momenta precludes the construction of a potential energy surface in the usual sense, it is possible, in time honored fashion [9,12], to compute zero-velocity curves which constitute an effective potential [13],

$$V(x,y) = K - \frac{1}{2}(\dot{x}^2 + \dot{y}^2) = -\frac{1}{r} - \frac{\omega^2(x^2 + y^2)}{2} + Fx, \quad (3)$$

where $\dot{x} = p_x + \omega y$ and $\dot{y} = p_y - \omega x$. The potential V has critical (equilibrium) points at $y = 0$ with x being given by the solutions of the cubic $\omega^2 x^3 - Fx^2 \pm 1 = 0$. There are four possible real critical points: If $0 < F < 3\omega^{4/3}/\sqrt[3]{4}$ only two real roots exist, x_+ (x_-), corresponding to a global maximum (saddle point) in the potential along the positive (negative) x axis. For $F > 3\omega^{4/3}/\sqrt[3]{4}$ two other positive roots appear but these do not correspond to physical maxima, minima, or saddles of the effective potential and can be ignored.

Since the motions for $F \neq 0$ will be referred to the synodic frame, we shall see what the motion for $F = 0$ (i.e., the hydrogen atom) looks like in the rotating system. This unorthodox view of the hydrogen atom is the natural starting point for studying the perturbed problem. The effective $F = 0$ potential, shown in Fig. 1(a), resembles the cone of a volcano with a circle of critical points lying along the rim given by $x^2 + y^2 = \rho^2 = \omega^{-4/3}$. Inspection of Fig. 1(a) suggests that stable motion (i.e., the bound states of the hydrogen atom) might be expected to be confined within the volcanic caldera and that exterior motion would be unstable. This interpretation would be incorrect: First, note that, in cylindrical coordinates (ρ, ϕ), the $F = 0$ potential *in the synodic frame*

$$\mathcal{V}(\rho, P_\phi) = \frac{P_\phi^2}{2\rho^2} - \frac{1}{\rho} - \omega P_\phi \qquad (4)$$

has a global equilibrium point—a saddle point—at $(\rho, P_\phi) = (\omega^{-2/3}, \omega^{-1/3})$ with $E_{eq} = -\omega^{2/3}$ where $P_\phi = \ell_z$ is conserved. An orbit with $E > E_{eq}$ is superimposed on the potential in Fig. 1(a) and is confined *above* the rim of the potential energy surface. In fact, the equilibrium in (ρ, P_ϕ) corresponds to the *rim* in the effective potential V in Fig. 1(a). Motion at or above the rim is stable provided $E < E_{ion} = -\omega P_\phi$, the ionization energy. Other stable orbits also exist having different P_ϕ values that lie both above and below the rim and correspond to local minima in $\mathcal{V}(\rho, P_\phi)$.

The location of an orbit and its particular ionization threshold are determined by E and also by the value of the Jacobi constant. For example, the "giant" bound orbit with $K = -2/5$ shown in Fig. 1(a) lies below the rim and is exterior to the caldera. While circular hydrogenic orbits remain circular in the rotating frame, elliptic orbits can assume quite complicated forms. For fixed K the eccentricity of an orbit is $e = \sqrt{1 - \ell^2/n^2}$, and, by this accounting, the giant exterior orbits are moderate to high eccentricity states, reflected by the (possibly substantial) variations in the electron's distance from the nucleus—see Fig. 1(a). The remarkable and counterintuitive behavior of these orbits can be explained by recalling that much of our intuition in this regard stems from the observation of Weierstrass [14] that stable motion is possible only at a potential minimum, but this holds *only* if the Hamiltonian can be split into the sum of a positive definite "kinetic" part depending quadratically on momenta and a "potential" part depending exclusively
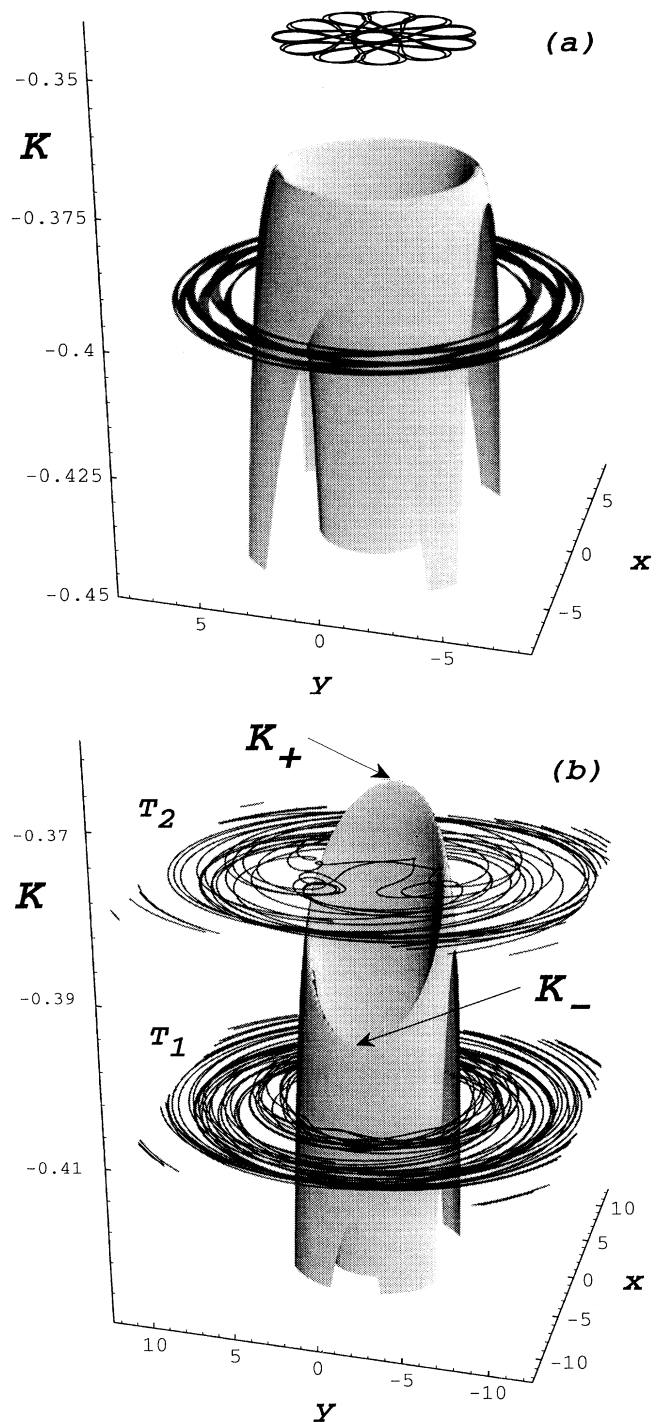

FIG. 1. Plots of $V(x, y)$ with typical orbits shown and $\omega = 1/8$. In (a) $F = 0$ and in (b) $F = 0.00342$. The orbit labeled T_2 in (b) eventually ionized.

on coordinates. Equation (2) does not satisfy this proviso, and the motion illustrated in Fig. 1 is permitted.

Numerical simulations confirm that as the CP field is turned on the initial distribution of orbits will contain some which are located inside the caldera, some outside,

and some above the rim shown in Fig. 1(a). The precise mix of the various kinds of orbit in the distribution depends sensitively on the details of the way in which the CP field is applied. Typically, the high eccentricity orbits that are preferentially prepared in a few-photon experiment are the most likely to evolve into the exterior giant orbits. As soon as F is changed from zero the global maximum and saddle point visible in Fig. 1(b) and located at x_+ and x_- are spawned. The values of the Jacobi constant at these two locations are denoted K_+ and K_-, respectively. It is clear from a comparison of Figs. 1(a) and 1(b) that mere visual inspection of zero-velocity curves is not sufficient to establish the onset of ionization. Rather, the stability of the critical points x_+ and x_- must be determined. To accomplish this we determined the eigenvalues of the symplectic vector space [8]. At the two critical points we find the following:

(i) x_-.—For $F > 0$ the four eigenvalues occur in pairs along the real and imaginary axes (i.e., $\pm\lambda_1, \pm i\lambda_2$ with $\lambda_{1,2}$ real) confirming that the motion corresponds to a saddle.

(ii) x_+.—For any $F > 0$ and $K < K_+$ the four eigenvalues occur in pairs along the imaginary axis. When $F = F_c = \frac{1}{2}(\frac{\omega}{3})^{4/3}$ and $K = K_+$ the eigenvalues collide in pairs and then march off into the complex plane as two sets of complex conjugates. This generally signals a transition from stable to unstable behavior similar to the Brown or Trojan bifurcation of the restricted three-body problem [8,9]. Thus, for $F < F_c$ and $K < K_+$ the maximum is, remarkably, *stable*, and seems to be the first example of this phenomenon to be recognized in atomic or molecular physics. Elsewhere we will argue that the range of stable motion at the maximum may be extended by application of a magnetic field perpendicular to the plane of polarization. Further, it is easy to verify that the critical points correspond only to $\ell_z > 0$ showing that these orbits will be the first to destabilize, accounting for the observed asymmetry in the effective ionization threshold between positive and negative ℓ_z states [13].

Typical surfaces of section are shown in Fig. 2 (for these surfaces $K_- = -0.3886$ and $K_+ = -0.3612$). Note that large regions of stable motion persist even above the threshold K_- as evidenced by the sets of foliated Kolmogorov-Arnold-Moser (KAM) curves that are labeled A and B. The A (B) KAM curves correspond to orbits of positive (negative) ℓ_z that, for $K < K_-$, are located *within* the caldera. Of course, these orbits do not conserve ℓ_z except in the $F = 0$ limit, but, for moderate fields, they do roughly conserve the sign of ℓ_z. As K is increased the orbits of negative ℓ_z remain stable while positive ℓ_z orbits destabilize by escaping across the saddle or maximum depending on the value of K. This is apparent in that the island labeled A is progressively eaten away as K is increased. For $K > K_+$ the A curves have vanished altogether. The B curves, on the other hand, remain stable despite their lying above the maximum in the effective potential.
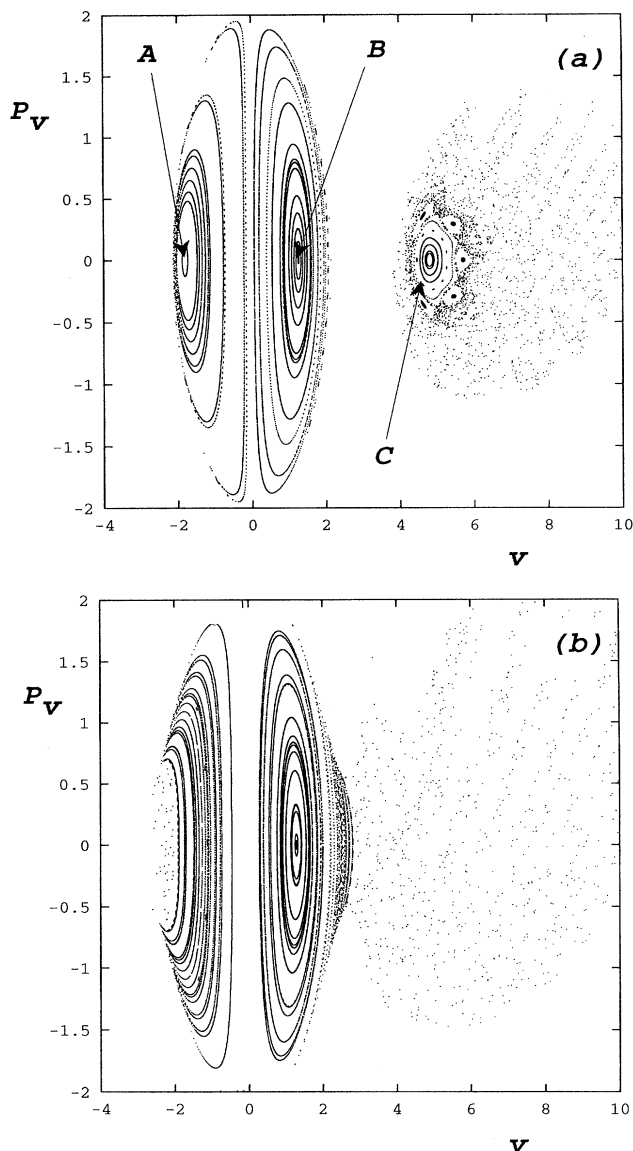

FIG. 2. Poincaré surfaces of section ($u = 0$) in parabolic coordinates; $x = (u^2 - v^2)/2, y = uv$, with $\omega = 1/8, F = 0.003\,42$ and (a) $K = -0.475$, (b) $K = -0.37$. For an explanation of the labels see the text.

The fate of the exterior, giant orbits illustrated in Fig. 1(b) and reflected by the island labeled C in Fig. 2(a) is crucial since these high eccentricity states may be populated extensively in an experiment. The giant orbits grow out of the $\ell_z > 0$ orbits in the $F = 0$ limit. As K is increased, a rapid transition to chaos occurs. However, if $K < K_-$, the orbits do not ionize—the motion is bound until the point at which $K = K_-$ when the ionization channel opens up. The mechanism is precisely the opposite of that observed for the interior orbits: Recent theoretical evidence, in fact, indicates that ionization occurs through a sequence of close encounters with the nucleus [15]. Only when $K \geq K_-$ are the chaotic,

eccentric giant orbits able to cross the saddle, thereby penetrating the caldera, undergoing close approaches to the nucleus and, subsequently, ionizing—see Fig. 1(b). Significantly, the giant orbits are the first to undergo a transition to chaos and, therefore, the apparent ionization threshold will be determined by the fraction of giants in the initial ensemble.

In conclusion, by examining the Hamiltonian flow we have established that while the ionization threshold corresponds to the saddle point in the effective potential, orbits, particularly circular orbits, may remain bound even though the saddle point or even the maximum are exceeded. This is, in part, due to the existence of an invariant discovered by Deprit [10]. Thus, it is possible to define a unique ionization threshold in the synodic frame below which no orbits will ionize, but individual orbits may be stable although their Jacobi constant exceeds the threshold value (compare Figs. 1 and 2). Thus the *observed* ionization threshold (e.g., expressed in terms of the percentage of orbits or atoms that ionize) will depend strongly on the details of the particular initial distribution of states that is prepared. The initial distribution in K is determined by both the manner in which the atom is excited and the way in which the CP field is turned on. This suggests a strong dependence of the apparent ionization threshold on state preparation. Indeed, the first thorough simulations of state preparation in these experiments is due to Kappertz and Nauenberg [6(c)] who found that the apparent (10%) ionization threshold is sensitive to the initial orbit parameters, such as the eccentricity, and the parameters of the field, such as the switch on time. Elucidation of the details of these and other issues in the light of these findings leaves considerable scope for future experimental and theoretical work. Finally we note that, after submission of this Letter, Bialynicki-Birula, Kaliński, and Eberly [16] have also described the Trojan bifurcation occurring at the maximum and investigated the quantum mechanical stability of Gaussian wave packets launched from that point.

[1] M. Gutzwiller, *Chaos in Classical and Quantum Mechanics* (Springer-Verlag, New York, 1990).

[2] J. E. Bayfield and P. M. Koch, Phys. Rev. Lett. **33**, 258 (1974).

[3] H. Hasegawa, M. Robnik, and G. Wunner, Prog. Theor. Phys. **98**, 198 (1989).

[4] G. Raithel, M. Fauth, and H. Walther, Phys. Rev. A **44**, 1898 (1991); G. Wiebusch *et al.*, Phys. Rev. Lett. **62**, 2821 (1989).

[5] P. Fu, T. J. Scholz, J. M. Hettema, and T. F. Gallagher, Phys. Rev. Lett. **64**, 511 (1990).

[6] (a) M. Nauenberg, Phys. Rev. Lett. **64**, 2731 (1990); (b) M. Nauenberg, Europhys. Lett. **13**, 611 (1990); (c) P. Kappertz and M. Nauenberg, Phys. Rev. A **47**, 4749 (1993).

[7] J. A. Griffiths and D. Farrelly, Phys. Rev. A **45**, R2678 (1992).

[8] R. Abraham and J. E. Marsden, *Foundations of Mechanics* (Addison-Wesley, Redwood City, CA, 1987), 2nd ed., pp. 675–688.

[9] A. Deprit and J. Henrard, Adv. Astron. Astrophys. **6**, 1 (1968); A. Deprit and A. Deprit-Bartholomé, Astron. J. **72**, 173 (1967).

[10] A. Deprit, in *The Big Bang and George Lemaitre*, edited by A. Berger (Reidel, Dordrecht, 1984), pp. 151–180; D. Farrelly and T. Uzer (to be published).

[11] A. Bohr and B. R. Mottelson, *Nuclear Structure* (W.A. Benjamin, Reading, MA, 1975), Vol. II; F. Mignard, Icarus **49**, 347 (1982).

[12] G. W. Hill, Am. J. Math. **1**, 5 (1878); V. Szebehely, *Theory of Orbits: The Restricted Problem of Three Bodies*, (Academic, New York and London, 1967). See especially Figs. 4.23 and 4.24.

[13] K. Rzazewski and B. Piraux, Phys. Rev. A **47**, R1612 (1993); A. Peregine-Smew, D. Farrelly, and T. Uzer (to be published).

[14] K. Weierstrass, in *Weierstrass: Mathematische Werke* (Berlin, 1894), Vol. 1, reprinted (Olms and Johnson, Hildesheim and New York, 1967), pp. 233–246.

[15] D. Farrelly, P. Bellomo, and T. Uzer (to be published); E. Lee, D. Farrelly, and T. Uzer, Chem. Phys. Lett. **231**, 241 (1994).

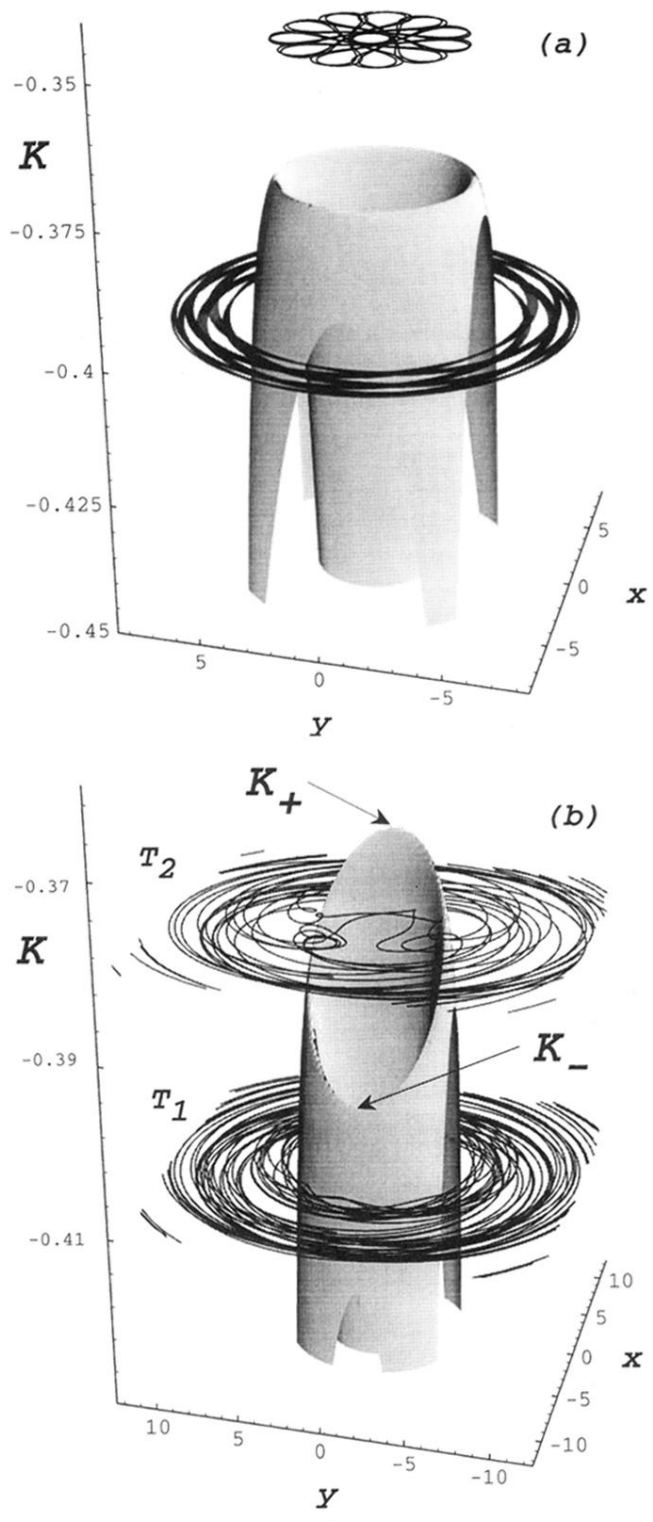[16] I. Bialynicki-Birula, M. Kaliński, and J. H. Eberly, Phys. Rev. Lett. **73**, 1777 (1994).

FIG. 1. Plots of $V(x,y)$ with typical orbits shown and $\omega = 1/8$. In (a) $F = 0$ and in (b) $F = 0.00342$. The orbit labeled T_2 in (b) eventually ionized.